Sensors and Materials, Vol. 32, No. 4 (2020) 1479–1487
MYU Tokyo

S & M 2195

Two-dimensional Thermoluminescence Dosimetry Using Al_2O_3:Cr Ceramics for 4, 6, and 10 MV X-ray Beams

Shin Yanagisawa,[1*] Daiki Maruyama,[1] Ryoken Oh,[1]
Yusuke Koba,[2] Takayuki Andoh,[3] and Kiyomitsu Shinsho[1]

[1]Tokyo Metropolitan University, 7-2-10 Higashi-Oku, Arakawa-ku, Tokyo 116-8551, Japan
[2]QST-NIRS, 4-9-1 Anagawa, Inage-ku, Chiba-shi, Chiba 263-8555, Japan
[3]Chiba Ceramic MFG Co., Ltd., 2-10-14 Inage-higashi, Inage-ku, Chiba-shi, Chiba 263-0031, Japan

(Received November 5, 2019; accepted February 4, 2020)

Keywords: radiotherapy, quality assurance, ceramic, dose distribution, 2D, passive dosimetry

Despite their advantages, two-dimensional (2D) thermoluminescence dosimeters (TLDs) have not yet replaced film dosimeters owing to their nonuniformity and low repeatability. A 2D TLD based on Al_2O_3:Cr ceramics is a promising new reusable passive dosimeter. 2D Al_2O_3:Cr TLDs can be used for geometry check tests and dose distribution verification in robotic radiosurgery using monoenergetic X-ray beams. In this work, the dependence of energy on the field size and water depth of 2D Al_2O_3:Cr TLDs for 4, 6, and 10 MV X-ray beams was investigated, because multienergy X-ray beams are used in radiotherapy. Intensity-modulated radiotherapy plan verifications were performed using the TLDs. The TLDs were found to have a large field size dependence for each energy, but their water depth dependence was small at a water depth above 4 cm for each energy. The relative dose distributions were verified with high accuracy using the TLDs.

1. Introduction

Dose distribution verification is important in high-precision radiotherapy, which can precisely deliver doses to tumors. Film dosimeters such as radiographic and radiochromic films are the most commonly used two-dimensional (2D) passive dosimeters for dose distribution measurement.[1–3] However, dose calibration and nonuniformity correction are difficult for film dosimeters because they are not reusable. Computed radiography (CR) plates using optically stimulated luminescence ($BaFSrBr:Eu^{2+}$ or $BaFBr_{0.85}I_{0.15}:Eu^{2+}$) have been reported as reusable 2D passive dosimeters for clinical applications of radiotherapy.[4,5] CR plates are useful imaging devices that can acquire highly uniform images with a short readout. However, they have a large energy dependence, so a lead filter must be used to minimize the over-response to low-energy photons. Owing to their large fading properties, the strict management of the decay time from irradiation to readout is required, and it is difficult to correct signal loss during irradiation. In addition, the introduction cost of the CR system is high for those who do not already have one for imaging.

*Corresponding author: e-mail: yanagisawa-shin@ed.tmu.ac.jp
https://doi.org/10.18494/SAM.2020.2698

ISSN 0914-4935
https://myukk.org/

Several 2D thermoluminescence dosimeters (TLDs) have been developed since the 1960s and are expected to be applied as reusable 2D passive dosimeters with a wide dynamic range.[6–12] In particular, tissue-equivalent 2D TLDs have been developed and used for clinical applications because of their small energy dependence. 2D TLDs have a potential advantage in being capable of correcting sensitivity nonuniformities for every pixel of acquired thermoluminescence (TL) images owing to their repeatability. However, most 2D TLDs do not have good repeatability because they contain resin as a base sheet or binder that causes sensitivity loss after repeated readouts.[13] In addition, it is difficult to produce 2D TLDs consisting of only tissue-equivalent TL phosphors. Hence, 2D TLDs have not been widely used as reusable 2D passive dosimeters.

Recently, we have developed a reusable passive 2D TLD based on Cr-doped Al_2O_3[14] (2D Al_2O_3:Cr TLD) that can acquire radiation images with high spatial resolution. Al_2O_3:Cr TLDs are robust and easy to handle. The repeatability obtained using a photomultiplier tube (PMT) system is well within 1% of the coefficient of variation (CV), and the dose response linearity ranges up to approximately 5 Gy for 6 MV X-ray beams.[12] The TL properties for charged particles have also been reported.[15,16] In addition, the use of water as a phantom material is standard for reference dosimetry in radiotherapy, and Al_2O_3:Cr TLDs can be used under water. A previous study suggested that 2D Al_2O_3:Cr TLDs have high applicability for the quality assurance of robotic radiosurgery.[17] However, Al_2O_3:Cr TLDs lack tissue equivalence. Also, multienergy X-ray beams are used in radiotherapy, while only 6 MV X-ray beams are used in robotic radiosurgery. Therefore, the X-ray energy spectrum changes with irradiation conditions, including the X-ray energy, field size, depth, and source-to-surface distance (SSD), and so does the TL efficiency. It is important to clarify the energy dependence of Al_2O_3:Cr TLDs for 2D TL dosimetry. The objectives of this study are to investigate the dependence of energy on the X-ray energy, field size, and water depth of Al_2O_3:Cr TLDs in radiotherapy and to demonstrate the use of TLDs in dose distribution verification.

2. Materials and Methods

2.1 2D TLD and 2D TL dosimetry

2D Al_2O_3:Cr TLDs with dimensions of 80 × 80 × 0.7 mm^3 were provided by Chiba Ceramic MFG Co., Ltd., in Japan. The Cr concentration was 0.034 wt%. The bulk density and effective atomic number of the TLDs were 3.7 g/cm^3 and 11.14, respectively. A prototype 2D TL reader[14] developed at Tokyo Metropolitan University consists of a dark box, an in-house developed hot plate, and a sensitive complementary metal-oxide-semiconductor (CMOS) camera (ORCA-Flash4.0 V2, C11440-22CU, Hamamatsu Photonics K.K., Japan). It can read 2D TLDs with dimensions up to 80 × 80 mm^2. 4, 6, and 10 MV X-ray beams from a TrueBeam® linear accelerator (Varian Medical Systems, USA) were used for irradiation experiments. The irradiated TLDs were held for 24 h under isothermal conditions at 5 °C in light-tight packages and read out by heating at 400 °C for 250 s. Since an integrated image is used, the temperature uniformity of the heater has little effect on the 2D TL dosimetry; however, the surface

temperature of the heater was maintained at 400 ± 3 °C. The 2D reader is described in detail in Ref. 18. TL images were acquired as TIFF images with a resolution of 50 μm/pixel by the image acquisition software High Performance Imaging System (HiPiC) (32-bit, version 9.2 pf5 12.03.2013, Hamamatsu Photonics K.K., Japan). The acquired TL images were processed using ImageJ (1.48v),[19] a public domain Java image processing program. Each TL response was an average in a circular region at the center of the irradiation field. The region diameter was 5.8 mm, which is the same as the total active length of the reference ion chamber (CC13, IBA Dosimetry, Germany).

2.2 Dose response curves

Dose response curves for 4, 6, and 10 MV X-ray beams were measured using the 2D Al_2O_3:Cr TLDs. The TLDs were placed under the reference condition, at a water depth of 10 cm using full-scatter solid water phantoms at an SSD of 90 cm. A 10-cm square irradiation field was used. For each energy, five dose levels of 100, 200, 300, 400, and 500 cGy were applied to water.

2.3 Field size dependence measurements

Output factors, which are the responses normalized by those with a 10 cm square field as a function of the field size, for 4, 6, and 10 MV X-ray beams were measured using the 2D Al_2O_3:Cr TLDs for field size dependence measurements. Figure 1 shows the irradiation geometry for the field size dependence. The TLDs were placed at a water depth of 10 cm using full-scatter solid water phantoms at an SSD of 90 cm. The sides of the square irradiation fields were 3, 4, 5, 7, and 10 cm. Each TL response for 250 monitor units (MUs) was compared with the reference value measured in water using an ion chamber (IC).

2.4 Water depth dependence measurements

Relative depth doses were measured using the TLDs. Figure 2 shows the irradiation geometry for the water depth dependence. The TLDs were placed at six water depths using full-scatter solid water phantoms at an SSD of 100 cm. The irradiation field was a 10 cm square. The water depths were 0, 2, 4, 7, 10, and 15 cm. Each TL response value for 250 MUs was compared with the reference value measured in water using the IC.

2.5 Dose distribution verification

An intensity-modulated radiotherapy (IMRT) plan using 10 MV X-rays from a Clinac® iX linear accelerator (Varian Medical Systems) was calculated using the Eclipse™ (version 13.6, Varian Medical Systems) treatment planning system (TPS). The maximum dose and pixel size of the plan were 211.9 cGy and 1.95 mm, respectively. Irradiation and dose distribution verification were performed three times using different TLD samples. The 2D Al_2O_3:Cr TLD

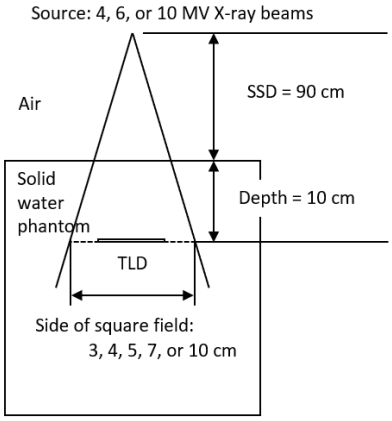

Fig. 1. Irradiation geometry for field size dependence of 2D Al_2O_3:Cr TLDs.

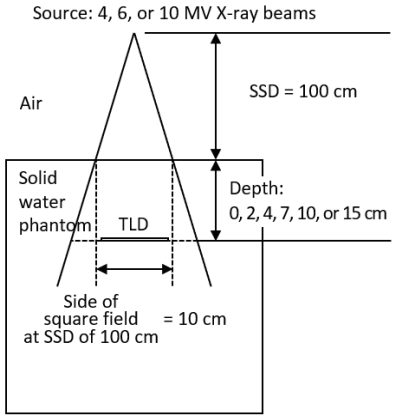

Fig. 2. Irradiation geometry for water depth dependence of 2D Al_2O_3:Cr TLDs.

was placed in the coronal plane at the center of the 30-cm-wide, 30-cm-long, and 20-cm-thick solid water phantom. The sensitivity of each pixel of the TLD was calibrated using the TL image for uniform irradiation with ImageJ. Figure 3 shows the dose response curve for the TLD. This was used to convert the calibrated TL images to dose distributions, and the DD-System (DD IMRT version 12.26, R-TECH.INC, Japan) analysis software was used for dose distribution verification. Each dose distribution from the TLD was compared with that calculated using the TPS with the gamma method, which evaluates both dose differences and dose-to-agreement (DTA). The acceptance criteria for dose differences and DTA were 3% and 2 mm, respectively.

3. Results and Discussion

3.1 Dose response curve

Figure 3 shows dose response curves of the 2D Al_2O_3:Cr TLDs for 4, 6, and 10 MV X-ray beams. The TLDs had high dose linearity up to 500 cGy for each X-ray energy. The dose response curves for 4, 6, and 10 MV X-rays were in good agreement, showing that the responses of the TLDs for 4, 6, and 10 MV X-rays under the reference condition are independent of energy. The CV for the three samples for each energy was determined to be approximately 4% at 100 cGy and within 2.5% above that. The CVs for the three energies at 100, 200, 300, 400, and 500 cGy were 4.7, 2.8, 1.8, 1.9, and 1.3%, respectively.

3.2 Field size dependence measurements

Figure 4 shows output factors measured using the 2D Al_2O_3:Cr TLDs and the IC for 4, 6, and 10 MV X-ray beams. For each X-ray energy, the TL responses decrease below the IC responses with decreasing side length of the square field (field size). The ratios of the output factors,

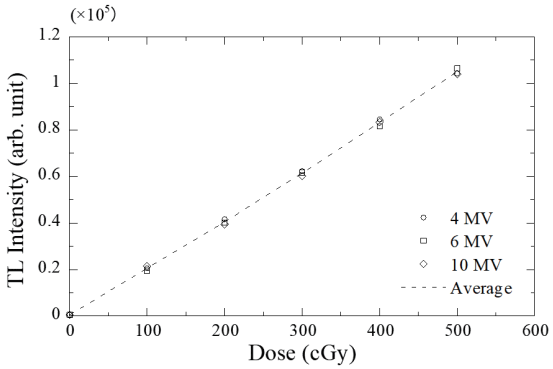

Fig. 3. Dose response curves of the 2D Al_2O_3:Cr TLDs for 4, 6, and 10 MV X-ray beams at water depth of 10 cm and SSD of 100 cm.

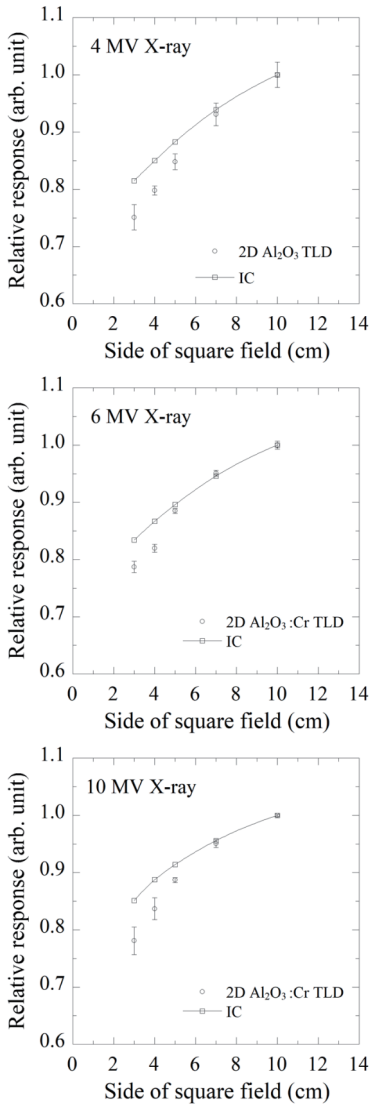

Fig. 4. Output factors for 2D Al_2O_3:Cr TLDs and IC for square fields with 3–10 cm sides for 4, 6, and 10 MV X-ray beams.

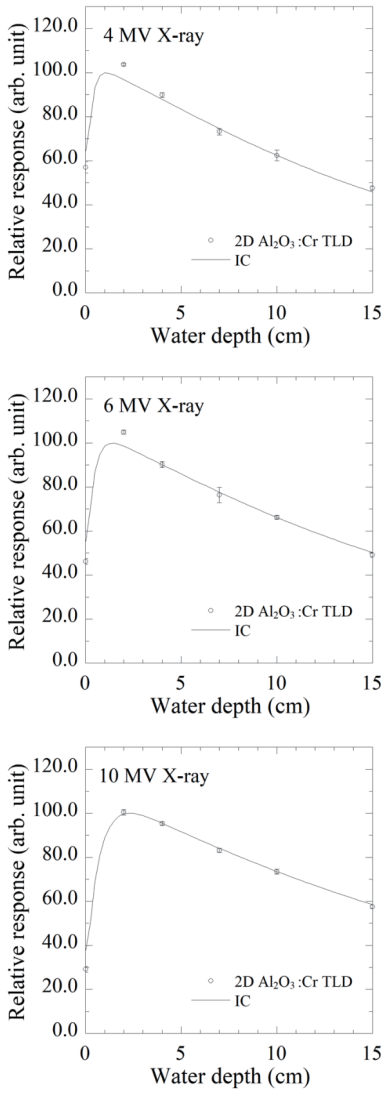

Fig. 5. Relative depth doses for 2D Al_2O_3:Cr TLDs and IC for square fields with 10 cm sides for 4, 6, and 10 MV X-ray beams.

namely, the TL responses to the IC response, are presented in Table 1. The ratio decreases by approximately 8% for a 3 cm side of the square field. The ratios of the mass energy absorption coefficient for Al_2O_3 to that for water are large for low-energy photons. In general, non-tissue-equivalent TLDs exhibit an over-response to low-energy photons owing to their mass energy absorption coefficient being larger than that of water. The proportion of low-energy photons decreases with decreasing field size.[20] Therefore, the ratio of output factor decreases with decreasing field size.

3.3 Water depth dependence measurements

Figure 5 shows relative depth doses measured using the 2D Al_2O_3:Cr TLDs with a 10 × 10 cm^2 field for 4, 6, and 10 MV X-ray beams. The relative depth doses of the TLDs were normalized with the IC response at a water depth of 10 cm and compared with those of the IC. The ratios of the relative depth doses, i.e., the TL responses to the IC response, are presented in Table 2. For each X-ray energy, the TLDs showed a large under-response at the surface. For the 4 and 6 MV X-ray beams, an over-response at a water depth of 2 cm was observed. However, for each energy, the relative response was consistent with those of the IC with a CV of approximately 2%. As described in Sect. 3.2, Al_2O_3:Cr TLDs exhibit an over-response to low-energy photons. The proportion of low-energy photons decreases with increasing water depth[20] and hence the ratio of relative depth dose increases with decreasing water depth.

3.4 Dose distribution verification

The IMRT dose distribution measured using a 2D Al_2O_3:Cr TLD and that calculated using the TPS are shown in Fig. 6. The spatial resolution of the dose distribution for the TLD was changed from the original spatial resolution of 50 μm/pixel to 0.65 mm/pixel to ensure it was sufficient for the spatial resolution of the treatment plan (1.95 mm/pixel). Figure 7 shows a dose profile comparison between the TLD and the TPS at the center of the dose distributions. The profiles of the TLD closely agree with those of the TPS. Since the spatial resolution of the dose distribution for the TLD is high, the dose profile at the penumbra for the TLD is steep compared with that for the TPS. The response ratio of the TLD to the TPS and the pass rate with criteria for a dose difference of 3% and a DTA of 2 mm for dose distribution verification with gamma

Table 1
Ratios of output factors for 2D Al_2O_3:Cr TLDs to IC for 4, 6, and 10 MV X-ray beams.

Side of square field (cm)	Energy		
	4 MV	6 MV	10 MV
3	0.921	0.943	0.918
4	0.939	0.946	0.943
5	0.960	0.988	0.971
7	0.992	1.005	0.994
10	1.000	1.000	1.000

Table 2
Ratios of relative depth doses for 2D Al_2O_3:Cr TLDs to IC for 4, 6, and 10 MV X-ray beams.

Water depth (cm)	Energy		
	4 MV	6 MV	10 MV
0	0.891	0.842	0.781
2	1.071	1.065	1.007
4	1.024	1.001	0.998
7	0.981	0.984	0.989
10	1.000	1.000	1.000
15	1.040	0.979	0.983

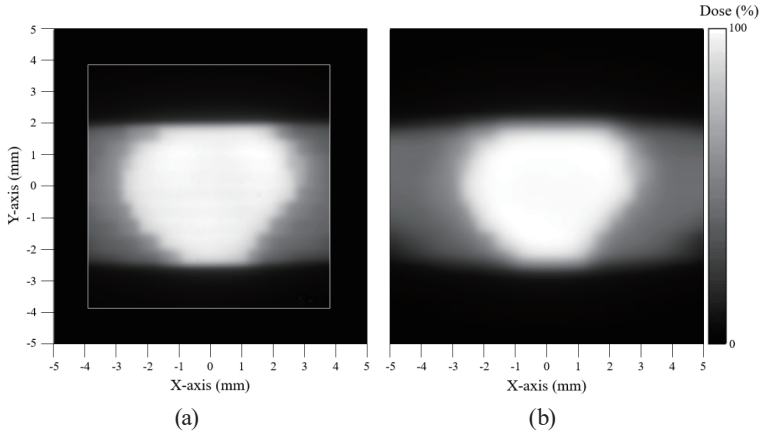

Fig. 6. (a) IMRT dose distribution measured using a 2D Al_2O_3:Cr TLD and (b) that calculated using the TPS.

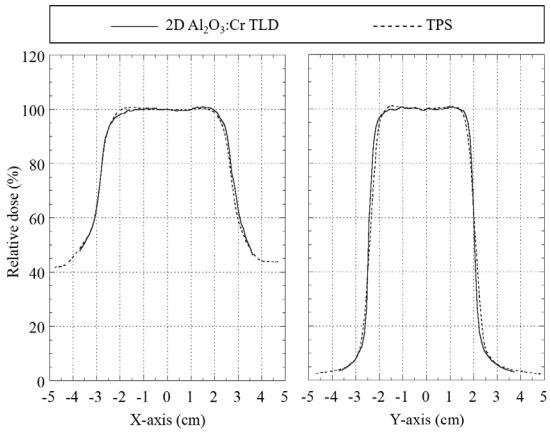

Fig. 7. Dose profile comparison between 2D Al_2O_3:Cr TLD and TPS.

Table 3
Gamma analysis results with acceptance criteria for dose difference of 3% and DTA of 2 mm for 2D Al_2O_3:Cr TLDs.

TLD No.	TLD/TPS (Arb. units)	Pass rate of gamma analysis (%)	
		Low dose threshold of 10%	Low dose threshold of 50%
1	0.916	82.27	94.03
2	0.847	82.06	94.49
3	0.933	83.45	94.41
Average	0.899	82.59	94.31

analysis for three TLDs are presented in Table 3. The average response ratio was 0.899 and the TLDs showed a large under-response because the IMRT field size is on the order of millimeters. The average pass rates with low dose thresholds of 10 and 50% were 82.59 and 94.41%, respectively. The dose difference was large at the penumbra, so the pass rates with a low dose threshold of 10% were smaller than those with a low dose threshold of 50%. This shows that we can perform relative dose distribution verification using a 2D Al_2O_3:Cr TLD with high spatial resolution.

4. Conclusions

We determined the field size and water depth dependences of 2D Al_2O_3:Cr TLDs for 4, 6, and 10 MV X-ray beams. We found that TLD response depends on field size and water depth. TL efficiency decreases with decreasing field size for each X-ray energy and increases with decreasing water depth for 4 and 6 MV X-ray beams, but it is almost constant at a water depth above 4 cm for each energy. We also demonstrated the dose distribution verification of an IMRT plan using the 2D Al_2O_3:Cr TLDs. We found that the 2D Al_2O_3:Cr TLDs had limited use for absolute dose measurement owing to their energy dependence. However, under the reference condition, absolute dose measurements could be performed within a standard uncertainty of 1.75%, and the relative dose distribution of an IMRT plan could be verified.

Acknowledgments

We thank Dr. Keisuke Sasai, Mr. Naoya Hara, and Mr. Akira Isobe for irradiation opportunities at the Juntendo University Hospital. This work was supported by JSPS KAKENHI grant number JP17J00046.

References

1 M. J. Butson, K. N. Yu, T. Cheung, and P. E. Metcalfe: Mater. Sci. Eng. R Rep. **41** (2003) 61. https://doi.org/10.1016/S0927-796X(03)00034-2
2 M. Fuss, E. Sturtewagen, C. D. Wagter, and D. Georg: Phys. Med. Biol. **52** (2007) 4211. https://doi.org/10.1088/0031-9155/52/14/013
3 S. Devic: Phys. Med. **27** (2011) 122. https://doi.org/10.1016/j.ejmp.2010.10.001
4 A. J. Olch: Med. Phys. **32** (2005) 2987. https://doi.org/10.1118/1.2012787
5 R. A. Day, A. P. Sanlar, W. H. Nailon, and A. S. MacLeod: Med. Phys. **38** (2011) 632. https://doi.org/10.1118/1.3525841
6 B. Marczewska, P. Bliski, P. Olko, and M. P. R. Waligórski: Radiat. Meas. **38** (2004) 833. https://doi.org/10.1016/j.radmeas.2004.03.014
7 K. Iwata, N. J. Yue, and R. Nath: Phys. Med. Biol. **49** (2004) 4049. https://doi.org/10.1088/0031-9155/49/17/015
8 N. Nariyama, A. Konnai, S. Ohnishi, N. Odano, A. Yamaji, N. Ozasa, and Y. Ishikawa: Radiat. Prot. Dosim. **120** (2006) 136. https://doi.org/10.1093/rpd/nci571
9 M. Kłoswski, L. Czopyk, K. Kisielewicz, D. Kabat, P. Olko, and M. P. R. Waligórski: Radiat. Meas. **45** (2010) 719. https://doi.org/10.1016/j.radmeas.2009.12.009
10 K. Shinsho, Y. Tomizawa, H. Horikawa, S. Miyajima, H. Saitoh, and A. Urushiyama: Radiat. Meas. **46** (2011) 1921. https://doi.org/10.1016/j.radmeas.2011.05.023
11 C. Kurokawa and A. Urushiyama: J. Phys. Conf. Ser. **444** (2013) 012035. https://doi.org/10.1088/1742-6596/444/1/012035
12 K. Shinsho, Y. Koba, G. Wakabayashi, S. Fukuda, R. Morimoto, D. Maruyama, H. Saitoh, and N. Sakurai: Radiat. Meas. **62** (2014) 15. https://doi.org/10.1016/j.radmeas.2014.01.001
13 M. Kłoswski, M. Liszka, R. Kopeć, P. Bilski, and D. Kędzierska: Radiat. Phys. Chem. **104** (2014) 212. https://doi.org/10.1016/j.radphyschem.2014.03.021
14 K. Shinsho, D. Maruyama, S. Yanagisawa, Y. Koba, M. Kakuta, K. Matsumoto, H. Ushiba, and T. Andoh: Sens. Mater. **30** (2018) 1591. https://doi.org/10.18494/SAM.2018.1928
15 Y. Koba, W. Chang, K. Shinsho, S. Yanagisawa, G. Wakabayashi, K. Matsumoto, H. Ushiba, and T. Ando: Sens. Mater. **28** (2016) 881. https://doi.org/10.18494/SAM.2016.1248
16 Y. Koba, R. Shimomura, W. Chang, K. Shinsho, S. Yanagisawa, G. Wakabayashi, K. Matsumoto, H. Ushiba, and T. Ando: Sens. Mater. **30** (2018) 1599. https://doi.org/10.18494/SAM.2018.1930
17 S. Yanagisawa, K. Shinsho, M. Inoue, Y. Koba, K. Matsumoto, H. Ushiba, and T. Andoh: Radiat. Meas. **106** (2017) 326. https://doi.org/10.1016/j.radmeas.2017.01.014

18 K. Shinsho, Y. Kawaji, S. Yanagisawa, K. Otsubo, Y. Koba, G. Wakabayashi, K. Matsumoto, and H. Ushiba: Appl. Radiat. Isot. **111** (2016) 117. https://doi.org/10.1016/j.apradiso.2016.02.020
19 C. A. Schneider, W. S. Rasband, and K. W. Eliceiri: Nat. Meth. **9** (2012) 671. https://doi.org/10.1038/nmeth.2089
20 H. Saitoh, T. Fujisaki, M. Fukushi, S. Abe, K. Fukuda, T. Katoh, H. Ootani, T. Irifune, and T. Hiraoka: J. Jpn. Soc. Radiol. Oncol. **11** (1999) 279. https://doi.org/10.11182/jastro1989.11.279